The Importance of Protein Size in Protein-Nanoparticle Interactions: From Protein Corona to Colloidal Self-Assembly

Laurent Marichal, Jéril Degrouard, Anouchka Gatin, Nolwenn Raffray, Jean-Christophe Aude, Yves Boulard, Sophie Combet, Fabrice Cousin, Stéphane Hourdez, Jean Mary, et al.

The Importance of Protein Size in Protein-Nanoparticle Interactions: From Protein Corona to Colloidal Self-Assembly

Laurent Marichal[a,b], Jéril Degrouard[c], Anouchka Gatin[a], Nolwenn Raffray[a], Jean-Christophe Aude[b], Yves Boulard[b], Sophie Combet[d], Fabrice Cousin[d], Stéphane Hourdez[e], Jean Mary[e], Jean-Philippe Renault[a], Serge Pin[a]**

[a]Université Paris-Saclay, CEA, CNRS, NIMBE, 91190 Gif-sur-Yvette, France

[b]Université Paris-Saclay, CEA, CNRS, I2BC, B3S, 91190 Gif-sur-Yvette, France

[c]Université Paris-Saclay, CNRS, Laboratoire de Physique des Solides, 91405 Orsay, France

[d]Université Paris-Saclay, Laboratoire Léon-Brillouin, UMR 12 CEA-CNRS, CEA-Saclay, 91191 Gif-sur-Yvette Cedex, France

[e]Sorbonne Université, CNRS, Lab. Adaptation et Diversité en Milieu Marin, Team DYDIV, Station Biologique de Roscoff, 29680 Roscoff, France

Corresponding Authors

Laurent Marichal*: marichal.laurent@hotmail.com

Serge Pin*: serge.pin@cea.fr

KEYWORDS

protein corona, self-assembly, protein size, nanoparticle, hemoglobin, adsorption

ABSTRACT

Protein adsorption on nanoparticles is an important field of study, particularly with regard to nanomedicine and nanotoxicology. Many factors can influence the composition and structure of the layer(s) of adsorbed proteins, the so-called “protein corona”. However, the role of protein size has not been specifically investigated, although some evidence has indicated its potential large role for corona composition and structure. To assess the role of protein size, we studied the interactions of hemoproteins (spanning a large size range) with monodisperse silica nanoparticles. We combined various techniques — adsorption isotherms, isothermal titration calorimetry, circular dichroism, and transmission electron cryomicroscopy — to address this issue. Overall, results show that small proteins behaved as typical model proteins, forming homogenous monolayers on the nanoparticle surface (protein corona). Their adsorption is purely enthalpy-driven, with subtle structural changes. In contrast, large proteins interact with nanoparticles *via* entropy-driven mechanisms. Their structure is completely preserved during adsorption and any given protein can directly bind to several nanoparticles forming bridges in these newly formed protein-nanoparticle assemblies. Protein size is clearly an overlooked factor that should be integrated in proteomics and toxicological studies.

TOC:

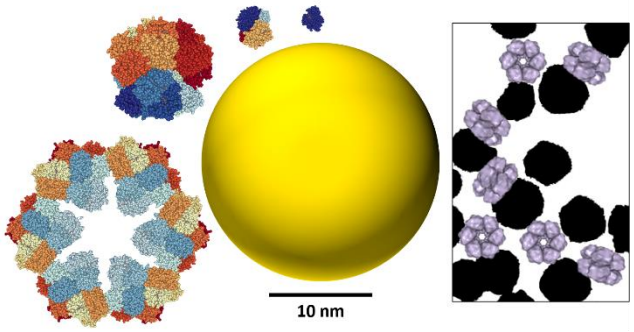

TEXT

Adsorption phenomena and, in particular, protein adsorption have been studied for more than a century.[1,2] Recently, protein adsorption has regained importance due to the development of nanoscience and nanotechnology,[3–5] and the subsequent manufacture of large amounts of engineered nanomaterials. Their applications are numerous in the environmental, agri-food, health, and pharmaceutical sectors. For example, nanoparticles (NPs) are used in medicines to prevent and treat diseases, including those used in vaccines, diagnostic probes, targeted drug delivery, material biocompatibility (implants), molecular imaging, and theranostic applications.[6–9] The field of nanotoxicology is concomitantly being developed to assess the risks and potential pernicious effects of exposure to NPs on health and the environment.[10–13] The main issue for the development of engineered NPs is the fact that, *in vivo*, NP physicochemical properties are usually totally distinct from their pristine state. In biological media, NPs are promptly covered by molecules (proteins, lipids, metabolites) that can bind to their surface and form a "biomolecular corona", giving NPs their biological identity.[14–17] The new entity can induce specific cellular recognition mechanisms causing cellular uptake, which strongly depends on the composition of the corona.[18–20] Moreover, it is now well established that the most studied type of interacting biomolecules — proteins — can induce deleterious biological effects by modifying their structure (often by partial loss of secondary structure),[21–23] and/or their function (protein activity can increase or decrease)[24–26] when adsorbed on NPs.

In a complex biological environment, many physicochemical factors can influence protein-NP interactions. A recent report established a comprehensive list of factors that have been shown to govern protein adsorption on NPs.[27] These factors are linked to the intrinsic properties of the NPs,

the adsorbed proteins, and the characteristics of their suspending medium, drawing the three sides of the nano-bio interface triangle.[28–30] Among all these physicochemical factors, some have been extensively studied, such as the size/curvature effect of NPs,[31–34] the physicochemical properties of protein sequences,[35–38] or the pH effect of the surrounding environment.[39–41] Others have not been as thoroughly examined, but may prove crucial in specific conditions (*e.g.*, NP roughness, dynamic flow, temperature).[42–44]

Non-covalent interactions of proteins with other molecules or with surfaces are often described in terms of electrostatic and hydrophobic interactions and, to a lesser extent, hydrogen bounds and Van der Waals forces.[45] A common way proteins can interact is through distortion of their internal structure. One model proposed by W. Norde predicts the adsorption or non-adsorption of proteins on a surface by using a relationship between the protein structural stability and its adsorption behavior.[21,46] In this context, proteins with low structural stability ("soft proteins") are preferentially adsorbed and their adsorption results in structural reorganization. On the contrary, proteins with a strong internal stability ("hard proteins") tend to not contribute to adsorption and, when they do, to not undergo any significant structural rearrangements. In more recent years, statistical comparative analyses[34,35,38] revealed that the main physicochemical factors relevant for protein adsorption on silica NPs include i) an enrichment in positively charged amino acids, particularly in arginine residues (forming electrostatic interactions with the negatively charged silica surface), and ii) an enrichment in disordered regions — and conversely a depletion in structured regions — confirming the hard/soft protein paradigm in the case of silica NPs.

Besides electrostatic interactions and disordered regions, protein size may also be an important parameter in determining corona composition. For instance, in coronas, there is an enrichment of high molecular weight proteins compared with their natural abundance in the medium.[34] This

result, as well as those from other studies done on flat surfaces,[47,48] point out the importance of protein size for protein adsorption. First, protein size has a large influence on adsorption kinetics, because small proteins get adsorbed faster (due to higher diffusion rates), but get replaced by larger proteins that can bind more strongly to the surface due to a larger contact area. This is one of the causes of the sequential adsorption mechanism called "Vroman effect",[49] and can have obvious consequences in terms of protein corona composition. Another effect caused by protein size is its correlation with adsorbent capacity.[47] Large proteins form thicker 3D interphases that separate the physical surface of the material from the bulk solution. Thus, these increased interfacial volumes can hold higher amounts of proteins compared to those formed by small proteins. Finally, a classification of proteins that combines Norde's paradigm with protein size has been proposed:[48] small and rigid proteins (*e.g.*, lysozyme, β-lactoglobulin) that behave as "hard proteins", intermediate-size proteins (*e.g.*, albumin, transferrin) being able to undergo conformational reorientations upon surface contact like "soft proteins", and high-molecular-weight proteins including lipoproteins and glycoproteins whose behavior is essentially dominated by the content of lipids or glycans. However, in this classification, protein size is not the only factor at play and no size effect can be extrapolated. Many studies comparing proteins of different sizes were not specifically designed to address this factor and used proteins with highly different physicochemical properties, such as isoelectric point, secondary structure, shape (globular or fibrillar), or dynamics. Therefore, a direct protein size effect cannot be established.

The aim of this study was to evaluate the effect of protein size on protein-NP interactions. The NPs used were spherical silica NPs whose size is commensurate with the proteins of interest (13.0 nm of radius). In order to unambiguously assess the protein size effect, this study was designed to satisfy three conditions: i) protein size is the only variable, ii) a size range as wide and relevant as

possible, and iii) well-characterized proteins. For these reasons, we chose proteins from the same family: hemoproteins. Their biochemical, functional, and structural properties are very similar to one another. They consist of varying numbers of subunits that possess a highly structured polypeptidic chain with a globin fold. To analyze the effect of protein size, we selected horse myoglobin (denoted Mb), pig hemoglobin (Hb), *Riftia pachyptila* coelomic hemoglobin (HbC1), and *Arenicola marina* hemoglobin (HbAm) which have molecular weights of 17, 65, 400, and 3600 kDa,[50–54] corresponding to radii of gyration of 1.4, 2.3, 6.0, and 11.0 nm, respectively. Interestingly, these hemoproteins respectively contain 1, 4, 24, or 144 similar subunits that can be considered as multimers of Mb (**Figure S1**). Overall, this size range covers almost every protein found in cells,[55] either in their free state or bound to protein complexes (*e.g.*, ribosomes, nucleosomes, *etc*.).

Adsorption isotherms, determined by solution depletion and by isothermal titration calorimetry, circular dichroism, and transmission electron cryomicroscopy experiments were combined to investigate the adsorption behaviors of proteins of different sizes, as well as the thermodynamics and structural consequences of their adsorption. With changes in both affinity constant, structural stability, and thermodynamic behavior, a protein-size effect could be established.

Results and Discussion

Protein and Nanoparticle Characterization

Table 1. Physicochemical characteristics of the hemoproteins used

	R_g [nm]	R_H [nm]	ζ potential pH 6 [mV]	ζ potential pH 7 [mV]	pH(I)
Mb	1.4 ± 0.1	2.4 ± 0.1	-1.8 ± 0.3	-4.0 ± 1.4	7.0 [56]
Hb	2.3 ± 0.2	4.1 ± 0.2	-1.3 ± 0.2	-3.5 ± 0.9	7.2 [50]
HbC1	6.0 ± 0.4	7.0 ± 0.1	-3.1 ± 2.1	-4.2 ± 0.3	N/A
HbAm	11.0 ± 0.4	17.8 ± 2.2	-6.1 ± 0.3	-11.3 ± 2.1	4.6 [57]
Silica NP	13.0 ± 0.2	33.6 ± 2.0	-11.3 ± 1.1	-17.1 ± 0.4	≈ 2 [58]

Radius of gyration (R_g), hydrodynamic radius (R_H), and zeta (ζ) potential of hemoproteins were measured in phosphate buffers (0.1 mol L^{-1}), at pH 6 and pH 7. Isoelectric points (pH(I)) taken from the literature are also indicated. Mb, horse myoglobin; Hb, pig hemoglobin; HbC1, *Riftia pachyptila* coelomic hemoglobin; HbAm, *Arenicola marina* hemoglobin. Standard deviations come from data fitting (R_g) or from the variability between replicates (R_H, ζ potential).

Prior to the experiments, the four hemoproteins were extensively characterized (**Table 1**). Hemoprotein samples were pure and presented the expected spectrophotometric and chromatographic characteristics (**Figures S2 and S3**). Using small-angle neutron scattering and based on the Guinier formalism, we measured their radii of gyration **(Figure S4**), which ranged from 1.4 to 11.0 nm. Their hydrodynamic radii, measured by dynamic light scattering, ranged from 2.4 to 17.8 nm. Zeta (ζ) potentials, measured by electrophoretic light scattering, at pH 6 and pH 7, were negative in every condition studied. The largest protein, HbAm, differed from the others by having larger negative values at both pH values. However, the mathematical model used for ζ potential calculation — namely the Smoluchowski approximation — assumes the presence of spherical objects.[59] This assumption is wrong in the case of HbAm which possess a particular hexagonal bilayer shape.[53,60] Thus, for HbAm, ζ potential determination is unreliable.

Mb, Hb, and HbC1 consist exclusively of Mb-like subunits (1, 4, and 24, respectively) and HbAm possesses 144 Mb-like subunits and 36 linker chains located inside the multimer that stabilize the global structure by forming non-covalent bonds with subunits.[60] Every Mb-like subunit has the same phylogenetic origin and, despite having a large variability of primary sequence, possesses a remarkably preserved globin fold that give them highly similar secondary and tertiary structures.[61,62] Thus, only the quaternary structure of the proteins (related to their multimeric state) differs.[63]

The silica NPs used were monodisperse LUDOX TM-50 nanospheres that were thoroughly characterized in our previous study (same batch).[64] Their size (radius of 13.0 nm) measured by small-angle neutron scattering (**Table 1 and Figure S5**) is commensurate with the size of the largest protein, HbAm. These NPs were chosen because they combine a small size and a low sensitivity to dissolution under our experimental conditions. Their negative ζ potentials confirm the acidity of silica[65] and indicate that the NP surface was negatively charged in the pH range of interest.

Adsorption Isotherms

The quantification of molecular interactions is essential to understand the physicochemical mechanisms at play. For instance, many techniques have been developed to assess binding affinity and stoichiometry in protein-protein interactions (*e.g.*, surface plasmon resonance, microscale thermophoresis, analytical ultracentrifugation).[66] However, each technique has limitations and only a combination of techniques can depict a complete picture of the situation. Here, to quantitatively assess the hemoprotein-NP interactions, we applied two adsorption isotherm techniques: solution depletion (**Figure 1**) and isothermal titration calorimetry (ITC, **Figures 2** and **S6** at pH 7 and 6, respectively). The first technique uses centrifugation to separate adsorbed

proteins from free proteins. This can lead to limitations related to weakly bound proteins or NPs and proteins having similar sedimentation coefficients.[16,67,68] The second technique measures the change in heat in a solution during titration. It does not require any labelling agent or separation step, but its drawbacks concern reactions not related to the interaction of interest or from its inability to probe athermic reactions.[69]

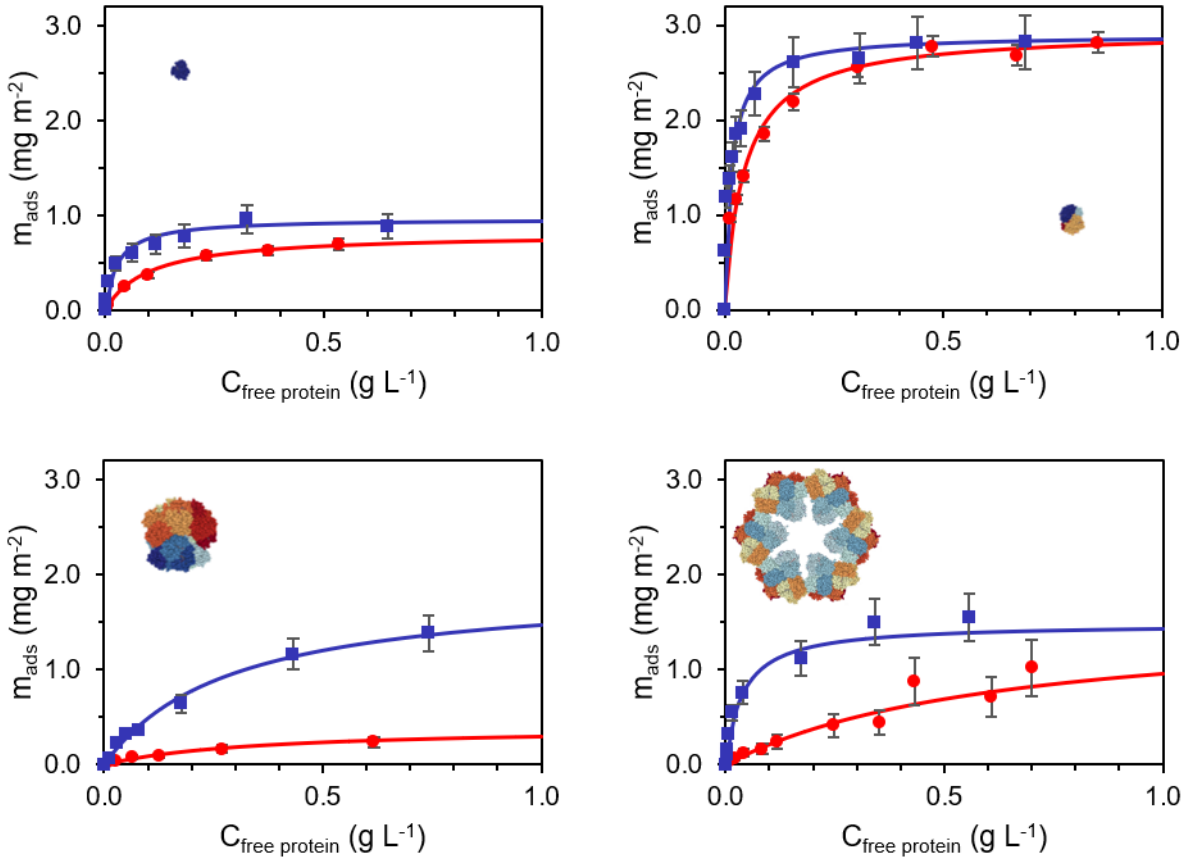

Figure 1. Adsorption isotherms of hemoproteins adsorbed on silica NPs: horse myoglobin (Mb) (Upper left), pig hemoglobin (Hb) (Upper right), *Riftia pachyptila* coelomic hemoglobin (HbC1) (Lower left), *Arenicola marina* hemoglobin (HbAm) (Lower right). Isotherms were performed in phosphate buffer (0.1 mol L^{-1}) pH 6 (blue squares) or pH 7 (red circles). For each condition, at least three replicas were done. The average values and standard deviations of the experimental

points are shown. Data were fitted using the Langmuir adsorption model (solid lines) calculated on averaged data.

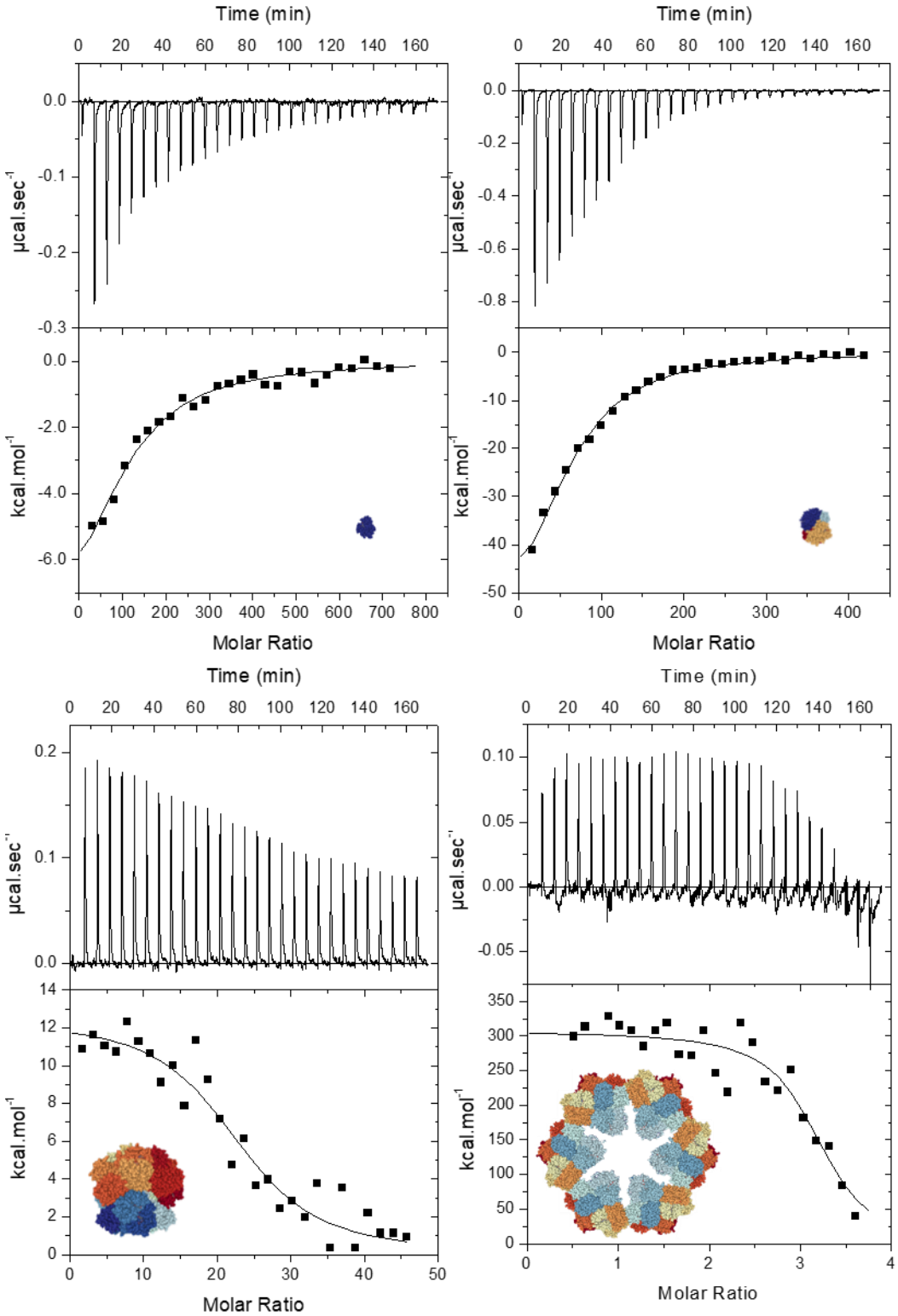

Figure 2. Isothermal titration calorimetry experiments of hemoproteins adsorbed on NPs in phosphate buffer (0.1 mol L^{-1}, pH 7): horse myoglobin (Mb) (Upper left), pig hemoglobin (Hb) (Upper right), *Riftia pachyptila* coelomic hemoglobin (HbC1) (Lower left), *Arenicola marina* hemoglobin (HbAm) (Lower right). Upper panels: raw data of the heat exchange. Each spike corresponds to one injection of protein solution in a NP solution. Lower panels: Integrated heat of each injection after subtraction of the dilution signal and titration curve fitted according to the SSIS model.

Table 2. Adsorption constants measured by isothermal titration calorimetry (ITC) (K_I) and solution depletion isotherms (K_{ads})

	pH 6			pH 7		
Protein	K_I [L mol^{-1}]	K_{ads} [L mol^{-1}]	K_I/K_{ads}	K_I [L mol^{-1}]	K_{ads} [L mol^{-1}]	K_I/K_{ads}
Mb	**2.9** ± 1.9 x 10^5	**5.4** ± 1.4 x 10^5	**0.5**	**1.6** ± 0.5 x 10^5	**1.7** ± 0.5 x 10^5	**0.9**
Hb	**5.9** ± 1.4 x 10^5	**4.0** ± 0.8 x 10^6	**0.1**	**6.8** ± 1.1 x 10^5	**1.9** ± 0.2 x 10^6	**0.4**
HbC1	**4.6** ± 2.5 x 10^6	**2.4** ± 0.3 x 10^6	**1.9**	**8.1** ± 3.2 x 10^5	**1.1** ± 0.7 x 10^6	**0.7**
HbAm	**3.7** ± 1.6 x 10^7	**8.3** ± 1.1 x 10^7	**0.4**	**5.2** ± 3.9 x 10^6	**5.7** ± 1.8 x 10^6	**0.9**

Measurements were taken in phosphate buffer (0.1 mol L^{-1}) at pH 6 and pH 7. Mb, horse myoglobin; Hb, pig hemoglobin; HbC1, *Riftia pachyptila* coelomic hemoglobin; HbAm, *Arenicola marina* hemoglobin. Standard deviations come from the variability between replicates.

Each hemoprotein-NP system was studied under two pH conditions (pH 6 and 7) to identify pH dependency. Adsorption constants, which are proportional to protein affinity, were deduced from these experiments (**Table 2**). In a number of cases, the values measured by ITC (K_I) and by solution depletion (K_{ads}) were quite different, K_I values being smaller than K_{ads} values. This can be explained by how proteins and NPs come into contact. With the solution-depletion technique, protein solution is added all at once, whereas with the ITC technique, the protein solution is added

sequentially. In the latter case, the nature of the NP surface evolves during the experiment with more and more proteins covering it. This leads to less favorable conditions for the adsorption of additional proteins due to repulsion effects between adsorbed and free proteins.[64] However, when comparing constants determined by the same technique, identical trends can be observed. The smallest protein (Mb) always had the weakest affinity, whereas the largest protein (HbAm) had the largest one, with up to two orders of magnitude between both values. Intermediate-sized proteins, Hb and HbC1, had intermediate affinities, not significantly different from one another. This pattern suggests that, if there is a trend between protein size and its affinity for NPs, other factors may also be at play.

The affinity values were always smaller at pH 7 than at pH 6, regardless of the protein. This difference can be explained by the change in surface charge under those pH values. With increasing pH, silica and hemoproteins had more negatively charged surfaces (**Table 1**). For silica, this is caused by the deprotonation of the main population of silanol groups that have a pKa of 5.6.[70] For hemoproteins, this change is due to their isoelectric point, which is either neutral or slightly acidic (**Table 1**). Between pH 6 and pH 7, histidine moieties are the only moieties whose charge can vary. Depending on their environment, their pKa ranges between 5 and 8[71] (*e.g.*, 6 out of 11 histidine moieties of Mb had a pKa comprised between 5.5 and 7).[72] Thus, at pH 7, histidine moieties are far less likely to be protonated (*i.e.*, positively charged) and thus to interact electrostatically with the negatively charged silica surfaces. This pH dependency indicates that electrostatic interactions promote hemoprotein adsorption on NPs. This was confirmed for Mb and Hb[40,73] and now can be extended to multimeric hemoglobins.

Table 3. Amounts of adsorbed protein per NP measured by isothermal titration calorimetry (ITC) (N_I) and solution depletion isotherms (N_{ads})

	pH 6			pH 7		
Protein	N_I [protein per NP]	N_{ads} [protein per NP]	N_I/N_{ads}	N_I [protein per NP]	N_{ads} [protein per NP]	N_I/N_{ads}
Mb	**32.2** ± 9.6	**265** ± 40	**0.1**	**87.7** ± 24.1	**226** ± 18	**0.4**
Hb	**95.9** ± 1.6	**210** ± 21	**0.5**	**73.4** ± 8.4	**212** ± 3	**0.4**
HbC1	**23.7** ± 1.9	**22.3** ± 2.4	**1.1**	**23.0** ± 1.7	**4.7** ± 1.1	**4.9**
HbAm	**1.7** ± 0.6	**2.0** ± 0.3	**0.9**	**3.2** ± 0.1	**2.1** ± 0.6	**1.5**

Measurements were taken in phosphate buffer (0.1 mol L^{-1}) at pH 6 and pH 7. Mb, horse myoglobin; Hb, pig hemoglobin; HbC1, *Riftia pachyptila* coelomic hemoglobin; HbAm, *Arenicola marina* hemoglobin. Standard deviations come from the variability between replicates.

The other constant measured by adsorption isotherm techniques was the stoichiometry (*i.e.*, the maximum number of adsorbed proteins per NP). Stoichiometries measured by ITC (N_I) and by solution depletion (N_{ads}) were generally quite different for any given condition (**Table 3**). For Mb and Hb, N_I values were always a small fraction of N_{ads} values (between 12% and 46%). This difference shows that a significant part (more than half) of hemoproteins are adsorbed by athermic phenomena or phenomena whose heat variations cancel each other out. This difference in stoichiometry has already been observed with proteins adsorbed on hydroxyapatite[69] and was attributed to the existence of two types of binding sites: sites with measurable enthalpy that are covered first and sites without measurable enthalpy. This interpretation empirically solves the problem, but the physical reasons of the site differences are still missing. In the present case, another athermic phenomenon can also be considered: hemoproteins mixed with silica NPs form aggregates.[64] Free proteins may then be trapped inside aggregates and be counted as adsorbed proteins, overestimating the actual amount of adsorbed protein indicated by the solution-depletion method. Nonetheless, these limitations compel us to be cautious when quantifying surface coverages. Remarkably, N_I and N_{ads} values of the large proteins, HbC1 and HbAm, were fairly consistent both at pH 6 and 7. The only exception was for HbC1 at pH 7 where N_I was 5 times

higher than N_{ads}, and identical to the values found at pH 6. In this case, the solution-depletion technique probably underestimated the stoichiometry. Due to pH effects, HbC1 interactions with NPs were weaker at pH 7 than at pH 6. Thus, this may be caused by a partial desorption of the adsorbed proteins during centrifugation.[74] If so, the centrifugation-based method becomes unsuitable for stoichiometry measurement and milder separation techniques (*e.g.*, chromatographic methods)[16,68] may be more appropriate. This doesn't necessarily apply to K_{ads} measurement. Indeed, K_{ads} is determined mainly by the slope of the isotherm and highly depends on the first points of the curve where all the NP surface is available. Despite being quite simple, silica surface has a mix of potential binding sites with different affinities.[65] The highest affinity sites are populated first and K_{ads} reflects their affinity. Proteins bound to high affinity sites will be less sensitive to centrifugation effect. In less favorable conditions (pH 7) the number of high affinity binding sites is likely reduced. However, this doesn't necessarily interfere in K_{ads} measurement as long as a significant amount of proteins still strongly interacts. This is evidenced by the lower but non-zero N_{ads} values at pH 7 compared to pH 6 for HbC1.

Comparing the N_{ads} values from the solution-depletion method, Mb and Hb adsorbed similar numbers of proteins on a NP surface (265 and 210 proteins per NP at pH 6, respectively). However, due to the larger size of Hb, there is actually a three-fold increase in terms of protein mass for Hb compared with Mb (**Figure 1**). This difference has already been observed under other physicochemical conditions (using the same method).[40,64] However, in both cases, a monolayer of adsorbed proteins formed, as confirmed by the hyperbolic shape of the isotherms (**Figure 1**), typical of a Langmuir adsorption model.[75] In contrast, HbC1 and HbAm, had smaller stoichiometries (≈ 23 and ≈ 2 proteins per NP, respectively). Using a simulation method developed

previously,[64,76] we calculated a theoretical maximal number of proteins per NP based on the coverage of a sphere by hard spheres of sizes similar to the hemoproteins. Up to 29 and 14 proteins (HbC1 and HbAm, respectively) can get adsorbed on the surface of each NP. Considering the necessary approximations of this comparison, HbC1 may be able to completely cover the NP surface, but HbAm is far from covering it.

Thermodynamics of Adsorption

ITC experiments (**Figures 2** and **S6**) also showed that small and large proteins interact on NPs with totally different calorimetric patterns, because the former had negative (exothermic) peaks and the latter had positive (endothermic) peaks (except for HbAm at pH 6). This difference translates into fundamentally distinct thermodynamic parameters (**Figure 3** for values at pH 7 and **Table S1** for values at both pH whose trends are comparable): small proteins have enthalpy-driven interactions (negative ΔH) and large proteins have entropy-driven interactions (negative $-T\Delta S$). During an adsorption process, variations in enthalpy can be associated with the number and strength of anchor residue contacts.[77] On the other hand, variations in entropy are more complex to interpret, but can be globally regarded as a measure of the configuration space of the particles.[78] Here, this configurational entropy had many components: conformational entropy (*i.e.*, the entropy associated with the number of distinct conformational states that are accessible to the surface-bound protein), translational and rotational entropies of the proteins, and buffer entropy (*i.e.*, the degree of freedom of water molecules and ions).[77–79]

Adsorption phenomena are both enthalpy- and entropy-driven, but one component usually predominates. In the case of Mb and Hb, the negative contribution of ΔS can be interpreted as a loss of conformational entropy confirmed experimentally for Mb adsorbed on silica NPs.[73] This loss of entropy is compensated by a gain in energy of the protein-NP complex in the form of

electrostatic interactions. There are a sufficient number of anchor contacts (electrostatic interactions) to keep the protein adsorbed. However, for HbC1 and HbAm, protein-surface electrostatic interactions, which are supported by the observed pH effects, were not the driving force and seem to not even compensate for the probable disruption of intra-protein interactions (as suggested by the positive *ΔH* values). The large increase in the entropy in these systems was clearly the driving force.

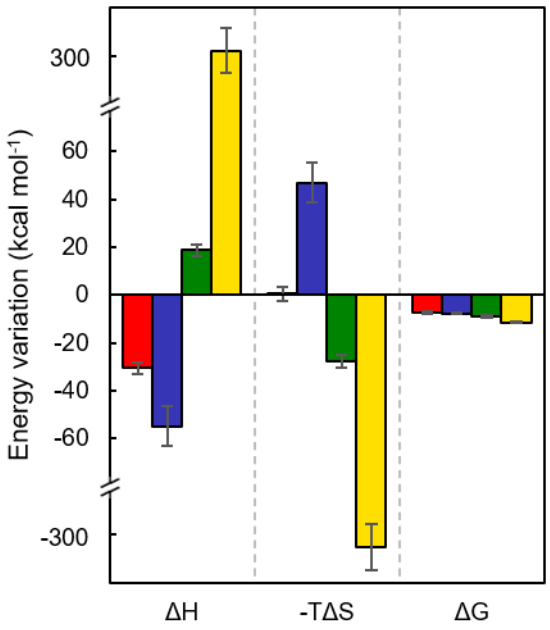

Figure 3. Thermodynamic values of hemoproteins adsorbed on silica NPs based on the ITC experiments done in phosphate buffer (0.1 mol L^{-1}, pH 7). Variations of free energy (*ΔG*), enthalpy (*ΔH*), and entropy (-T*ΔS*) for horse myoglobin (Mb) (red), pig hemoglobin (Hb) (blue), *Riftia pachyptila* coelomic hemoglobin (HbC1) (green), *Arenicola marina* hemoglobin (HbAm) (yellow). Each value is the average of three replicates.

We can distinguish local molecular entropic effects from global ones. Among local effects, the first entropy-driven mechanism is the destructuration of proteins, either by multimeric disassembly or by unfolding. This explanation has a long history in protein adsorption.[46] In addition, one can also mention an increase in solvent entropy due to the expulsion of ions and water molecules ordered at the surface. This is the origin of hydrophobic interactions and is also at play during adsorption.[46] It has been shown with peptides and proteins adsorbed on charged surfaces that, in some cases, solvent entropy gains can be larger than the decrease in conformational entropy of the bound molecule.[79,80] Also, there is a direct link between protein size and the number of water molecules that can be displaced during adsorption.[47] Thus, for large proteins such as HbC1 and HbAm, the increase in solvent entropy may dominate even more. We can also classify the so-called chelate effect as a local effect. Although it has not been described as a chelate effect, prestructuration of large multimeric proteins may induce similar positive cooperativity phenomena: preexisting bonds cancel the entropic penalty of new bonds.[81] Both HbC1 and HbAm are highly multimeric and have many intra- and inter-helix interactions, especially disulfide and ionic bonds formed by divalent cations,[54,60] that are not present in Mb and Hb.[50] Applied here, a chelate effect may explain both the high affinity of HbC1 and HbAm for NPs and the entropic nature of their adsorption on NPs.

Finally, global effects give rise to the so-called entropic forces in colloidal sciences.[82] Colloid studies have revealed many entropy-driven transitions from disorder to order.[78] In particular, the depletion interaction, which is fundamentally entropic, may play a role: when two large particles come nearer to each other, they create more space for the other particles to move, increasing the total entropy of the system.[78]

Structural Studies

Among all these possible explanations, some can be tested using structural analyses. To examine potential structural changes upon adsorption, UV circular dichroism (CD) experiments were performed on free and adsorbed hemoproteins (**Figure 4**). Each free hemoprotein had a similar CD spectrum characterized by a maximum at about 192 nm and two minima at 208 and 222 nm (**Figure S7**). This pattern is typical of α-helix-rich proteins with the 192 and 208 nm bands corresponding to the $\pi \rightarrow \pi^*$ excitation transition (perpendicularly and parallel-polarized, respectively) and the 222 nm band corresponding to the $n \rightarrow \pi^*$ transition.[83,84] The comparison between free and adsorbed proteins shows different behaviors between the systems. The large proteins, HbC1 and HbAm, did not exhibit any significant differences between adsorbed and free proteins. However, the two small proteins, Mb and Hb, had weaker CD signals in the 208 and 222 nm regions for the adsorbed proteins, the decrease being much stronger in the 208 nm region. Based on instrumental limitations, no conclusion can be drawn for the 192 nm region.

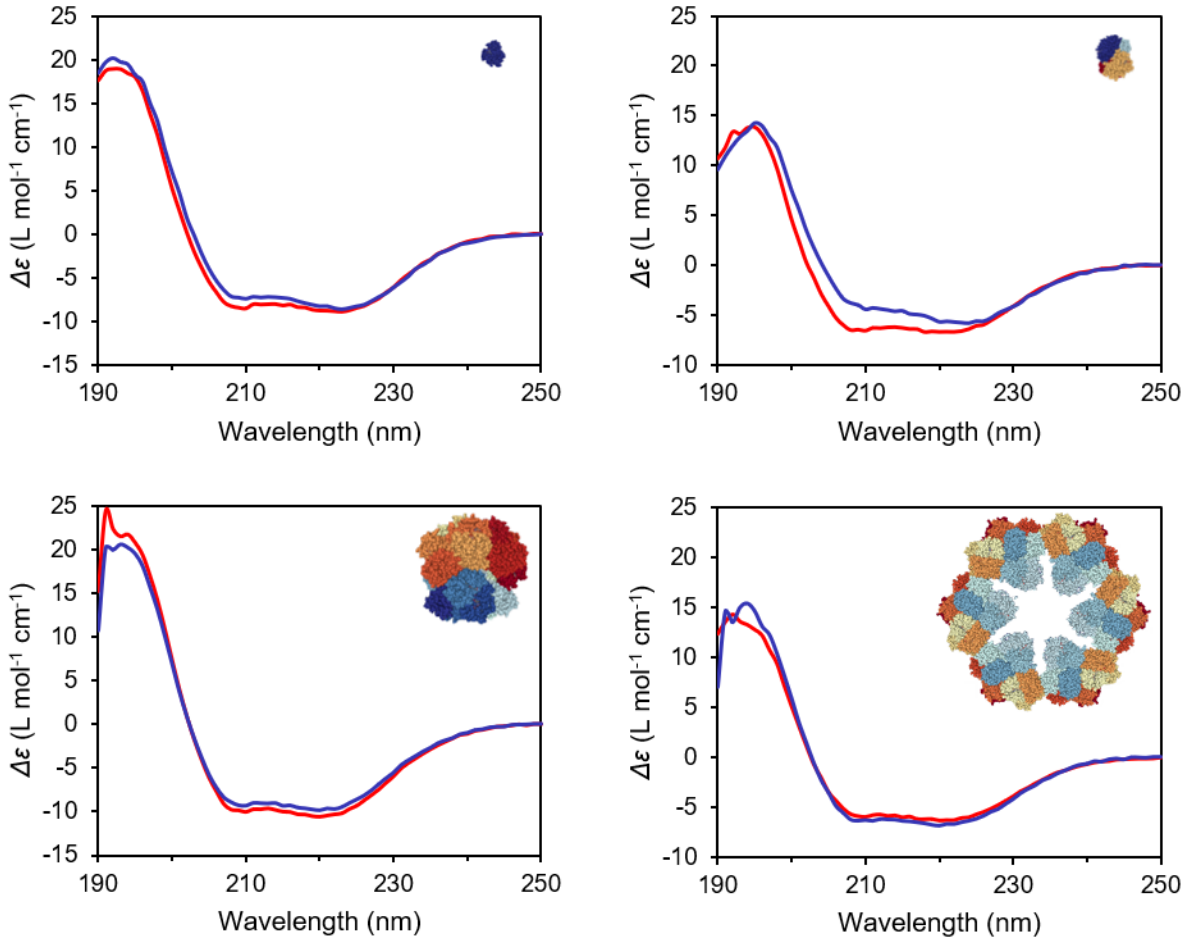

Figure 4. Circular dichroism spectra of hemoproteins, free in solution (red lines) or adsorbed on silica NPs (blue lines) in phosphate buffer (0.1 mol L^{-1}, pH 7). $C_{subunit}$ = 3 µmol L^{-1}. C_{NP} varied between 1 and 20 g L^{-1}.

Table 4. r_α (θ_{222}:θ_{208}) ratios of hemoproteins, free in solution or adsorbed on silica NPs.

Protein	r_α - free proteins	r_α - proteins and NPs
Mb	**1.08** ± 0.01	**1.27** ± 0.17
Hb	**1.04** ± 0.01	**1.51** ± 0.10
HbC1	**1.06** ± 0.02	**1.05** ± 0.06
HbAm	**1.09** ± 0.02	**1.10** ± 0.03

Values are the average of at least three independent replicates. Mb, horse myoglobin; Hb, pig hemoglobin; HbC1, *Riftia pachyptila* coelomic hemoglobin; HbAm, *Arenicola marina* hemoglobin. Uncertainty values (standard deviations) come from the adjustment of experimental data and from the use of replicates.

To quantify the dichroism discrepancy, we calculated the r_α (θ_{222}:θ_{208}) ratios (**Table 4**). Free hemoproteins had similar r_α values (between 1.04 and 1.09), but adsorbed proteins had very different r_α values. HbC1 and HbAm kept the same r_α values when adsorbed. However, Mb and Hb had significantly higher r_α values (1.27 and 1.51, respectively) compared with free proteins. The r_α ratio has been used to distinguish between two structural states of α-helix peptides,[85–88] non-associated helices (for $r_\alpha \leq 1$) and coiled-coil systems (for $r_\alpha > 1$). Applied to hemoproteins, a coiled-coil formation seems unlikely. After adsorption, Mb-like subunits keep their tertiary structure[64,73] and the linker chains of HbAm, which already have a coiled-coil conformation, are located inside the multimer.[60] However, the change in r_α may be caused by conformational changes happening in the α-helix structure as suggested for tropomyosin.[89] In our case, we hypothesize that a loss and/or rearrangement of the protein hydrogen bond network occurs when hemoproteins get adsorbed. This rearrangement leads to helix-NP surface interactions and possibly to new helix-helix interactions. Therefore, for small proteins, conformational changes seem to occur and may be connected to functional changes (oxygenation properties) previously seen on Hb adsorbed on NPs.[26,40,64] However, this should not be regarded as destructuration, because the changes are subtle and do not lead to a loss of shape or function.[64] For large proteins, the lack of differences can be explained by the fact that only a small number of subunits are in direct interaction with the NP surface and thus get rearranged.

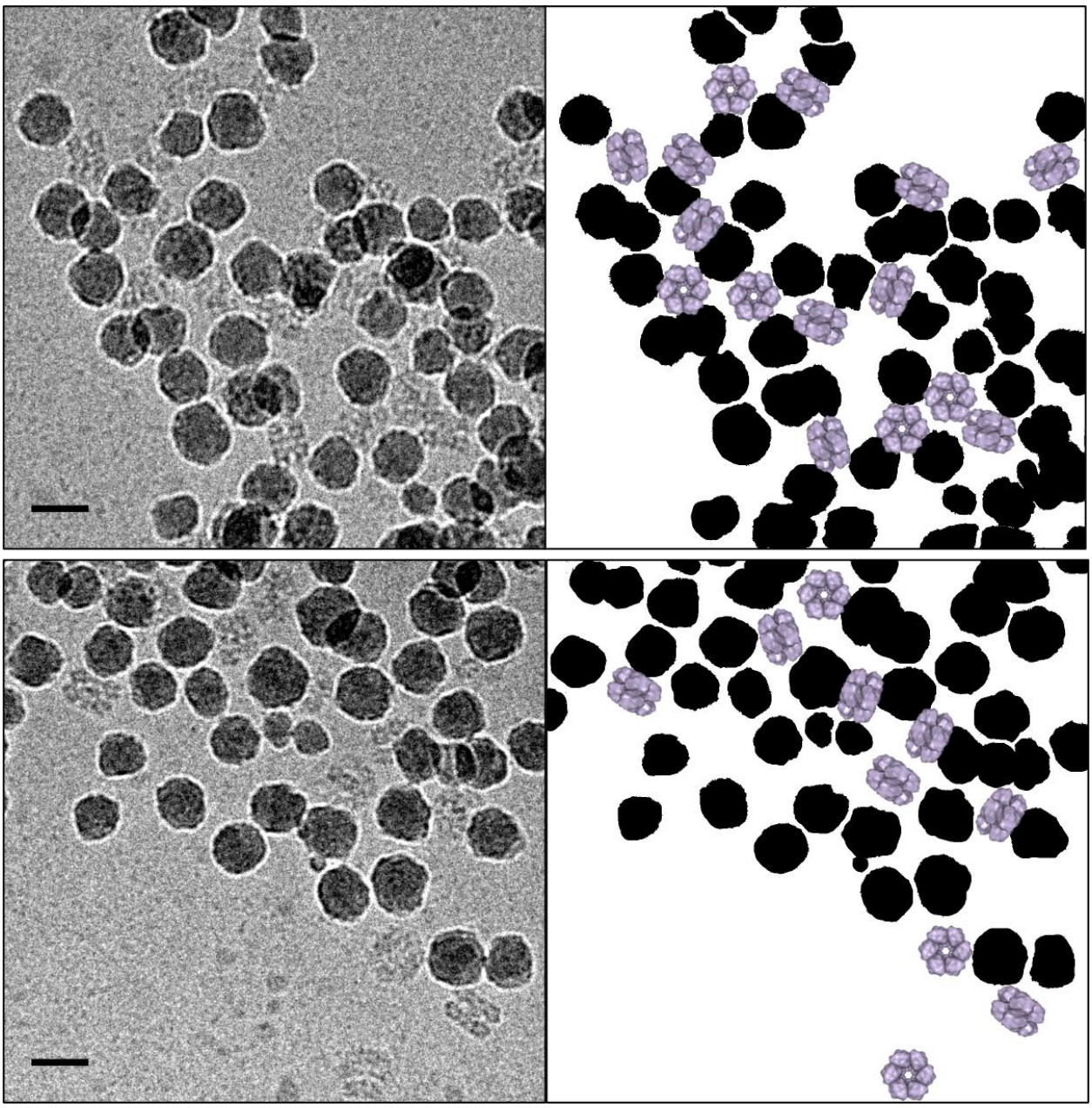

Figure 5. Cryo-TEM micrographs of HbAm proteins adsorbed on silica nanoparticles (NPs) in phosphate buffer (0.1 mol L^{-1}) at pH 6 (top) and 7 (bottom). The corresponding schematics highlighting the orientation of the proteins (in purple) relative to the NPs (in black) are also given. C_{HbAm} = 0.4 g L^{-1}, C_{NP} = 3 and 6 g L^{-1} (pH 6 and 7, respectively) to obtain more than 80% of adsorbed proteins. Scale bars: 30 nm.

Nevertheless, multimeric proteins may undergo disassembly processes that cannot be probed using CD. The structure of adsorbed HbAm was thus assessed by taking cryo-TEM images of HbAm adsorbed on NPs at pH 6 and pH 7 (**Figure 5**). In both cases, the typical hexagonal bilayer shape of the protein was maintained (**Figure S1**)[53] even when the protein was adsorbed. This eliminates the hypothesis of subunit dissociation or large destructuration upon adsorption. In addition, we can be more specific about the type of self-assembly observed here. HbAm and NPs form open network structures.[90] NPs did not seem to interact with more than two proteins (based on a sample of seven images for each pH value). This is in agreement with the stoichiometries found by isotherms and confirms the incomplete coverage of the surface by HbAm. Conversely, each HbAm protein could interact with up to four NPs. In this case, we can even consider that NPs are adsorbed on proteins, because HbAm and NPs have very similar sizes. In this network, much of the NP surface is not available for any additional protein adsorption due to steric effects, thus possibly explaining the very low stoichiometry values. Moreover, at pH 6, HbAm seemed to interact with more NPs (up to 4 NPs per protein) than at pH 7, resulting in a higher aggregation state and confirming pH dependency. Finally, at both pH value, proteins did not have specific orientations towards NPs. The binding site can be located either on one of the faces (near the "hole"), on the side, or on one of the edges of the protein (**Figure S8**). This nonspecific orientation suggests that HbAm do not maximize their interaction with the NPs. The chelate effect and the water expulsion hypotheses are thus unlikely.

Therefore, having ruled out all local entropic considerations, we are left with the global entropic explanation based only on the colloidal nature of the protein observed here. The nearest connection is the physics of patchy colloids that can form open networks.[91] The current understanding of the

entropic forces underlying such lattices is the conservation of a maximum degree of rotational entropy.

These results, as well as previous results,[26,40] show that adsorption on negatively charged NPs is not detrimental to the native structure of hemoproteins, inducing only subtle structural rearrangements, and preserving their biological oxygen-carrying function, which depends strongly on tertiary and quaternary structures. Moreover, cryo-TEM images, as well as small-angle neutron scattering experiments done with Mb and Hb interacting with NPs[64] clearly showed that hemoprotein-NP interactions lead to reaction-limited aggregation mechanisms. Many studies have experienced NP aggregation in presence of proteins caused by unfolding of proteins during adsorption.[92–94] This NP aggregation phenomenon implies that protein unfolding can induce protein-protein interactions, linking the NPs *via* their respective coronas. Here, protein-induced NP assembly is clearly not caused by protein unfolding, but by proteins bridging the NPs, *i.e.*, the same protein can belong to two (or more) coronas forming an open network of proteins and NPs. Although every hemoprotein seems to form networks, their exact structure is not known and may differ depending on their size (formation of more or less close-knit networks). Additional studies using cryo-TEM or small-angle scattering would be very useful to determine if other lattices can be formed under specific conditions.

Finally, based on these results, the classification of proteins between three classes (small and hard proteins, intermediate and soft proteins, and high molecular weight proteins) proposed by Rabe *et al*.[48] should be reconsidered. Hemoproteins of any size are highly structured and don't suffer any large structural modifications during adsorption. Then, none of them belong to the soft protein class despite covering the intermediate size range. Moreover, the high molecular weight protein class is said to be determined by the content of lipids and glycans. None of them are present

in the hemoproteins studied (including the very high molecular weight HbAm). Eventually, based on their structural stability, the four hemoproteins studied should fit in the hard protein class. Then, the small size attributed to the hard protein class becomes wrong. Therefore, none of the classes should be defined in terms of size and larger-scale studies should be designed in order to refine this classification.

Conclusion

The present study demonstrated the existence of a protein-size effect in the case of hemoproteins adsorbed on silica NPs. Large proteins tend to interact with more affinity for NPs than small proteins. This may be of great importance when considering protein corona formation in complex biological media where large proteins complexes are present. Until recently,[34] proteomics studies had not identified protein size as a determining factor for protein adsorption. This is partly due to the fact that proteins are usually considered in terms of amino-acid sequences and that the actual protein size (or protein complex size) cannot be computationally investigated by classical proteomics analyses.

We highlighted the fact that both techniques used to perform the isotherms have their limitations that need to be acknowledged before any interpretation. Adsorption isotherms by solution depletion are not well suited for weakly bound proteins. If this is the only isotherm technique used, it would be of interest to quantify the binding strength of a given system using analytical centrifugation.[67] On the other hand, calorimetric isotherms are intrinsically limited by the fact that all thermodynamic variations of a system are measured at the same time and that some of them cancel each other out, concealing part of the information. A combination of techniques is definitely the best approach to overcome these limitations.

Calorimetry experiments clearly showed that closely related proteins can have fundamentally different thermodynamic behavior in adsorption, with small proteins adsorbing *via* enthalpy-driven phenomena (*i.e.*, electrostatic interactions) and large proteins adsorbing *via* entropy-driven phenomena (several possible causes). Entropy-driven adsorption may be common for very large proteins or protein complexes, which may behave as colloids.

Contrary to homogenous protein coronas formed by typical model proteins, large proteins tend to form incomplete coronas. This can be easily explained by the fact that large proteins are more likely to bind to several NPs causing the self-assembly of aggregated structures that prevent more proteins from interacting with the empty surface due to steric effects.

Finally, each hemoprotein keeps its overall (quaternary) structure during adsorption. However, subtle changes in the tertiary structure (*i.e.*, organization of helices) occur for small proteins, but not for large ones. These changes may explain the modifications in oxygenation properties found for Hb adsorbed on silica NPs.[26,40,64] The absence of any structural impact for large proteins may also be of great interest for the design of hemoglobin-based oxygen carriers.[26]

Experimental Procedures

Chemicals

Phosphate buffers were prepared by dissolving disodium phosphate (28029 VWR Chemicals, purity ≥ 99.5%) and monosodium phosphate (28015 VWR Chemicals, purity ≥ 99%) salts in pure, Milli-Q water (MilliPore, 18 MΩ cm).

Silica nanoparticles (LUDOX® TM-50, Merck) are nanospheres with a physical radius of 13.0 ± 0.2 nm[64]. Shortly before the experiments, NPs were dialyzed twice against 100 volumes of pure water for a minimum of 3h per dialysis to eliminate excess salts (using Spectra/Por™ 3.5 kDa

dialysis membranes). The suspension was then filtered using a 0.45 µm syringe filter (Sartorius) and the NP mass concentration was measured by desiccation (90°C, overnight) of 1 mL aliquots and dry mass weighing.

Protein Preparation

Metmyoglobin from equine heart (Mb) was purchased as a lyophilized powder (M1882, Merck), solubilized, dialyzed twice against 100 volumes of pure water at 4 °C, and centrifuged (20,000 g) for 10 min before use. The Mb concentration was measured by spectrophotometry with ε_{623} = 3500 L mol^{-1} cm^{-1}.[50]

Pig hemoglobin (Hb) was purified in its oxygenated form from fresh blood following standard preparation[95] using erythrocyte membrane precipitation. Then, the Hb solution was dialyzed three times against 100 volumes of pure water at 4 °C, stripped of the bound 2,3-diphosphoglycerate by passing the desalted hemoglobin solution through a mixed-bed ion-exchange resin (AG® 501-X8, Bio-Rad), and centrifuged at 20,000 g for 10 min[96]. The Hb concentration was measured using spectrophotometry with ε_{576} = 15,150 L mol^{-1} cm^{-1}.[50]

Extracellular hemoglobins were purified from biological fluids given by the Roscoff Marine Station (France). *Riftia pachyptila* coelom was collected during an oceanographic expedition on the East Pacific Rise (MESCAL 2011) and stored at -80 °C until use. *Arenicola marina* blood was collected from specimens harvested on the shore in Roscoff (France). The purification process was adapted from protocols developed previously.[51,53] Briefly, fluids were centrifuged twice (20,000 g, 10 min, 4 °C) to eliminate suspended particles, then eluted in a Superose® 6 Increase 10/300 column (GE Healthcare) using an ÄKTA FPLC system for size-exclusion chromatography. The elution was followed by spectrophotometry at 280 nm (all proteins) and 414 nm (hemoproteins only). The fractions of native hemoproteins were the largest and the first to be eluted (due to their

large size) and were isolated and pooled (**Figure S3**). The pooled fractions were then concentrated using 100 kDa Amicon Ultra-4 units (Merck), and stored at 4 °C. To our knowledge, no molar extinction coefficient (ε) had been established for *R. pachyptila* coelomic hemoglobin (HbC1) or *A. marina* blood hemoglobin (HbAm). Measurements of the amount of iron atoms using inducted coupled plasma mass spectrometry on an iCAP Q (Thermo Scientific) allowed us to deduce ε values at the Soret band: ε_{414} = 170,000 and 160,000 L mol^{-1} cm^{-1} for HbC1 and HbAm, respectively (data not shown). Absorption spectra of every hemoprotein are given in **Figure S2**.

After purification, protein solutions were thoroughly characterized in order to check for purity and for physicochemical assessment. Hydrodynamic radii (R_H) and zeta (ζ) potentials were measured using a Zetasizer Nano ZS (Malvern Instruments). Samples were placed in phosphate buffers (0.1 mol L^{-1}), at pH 6 or pH 7 and measurement were done in triplicate. Radii of gyration (R_g) were measured using small-angle neutron scattering following the method developed previously.[64] Samples were placed in 100% D_2O phosphate buffer (0.1 mol L^{-1}, pD 7).

Adsorption Isotherms

Adsorption isotherms of hemoproteins on silica NPs were measured using a centrifugation-based solution-depletion method (amount of adsorbed proteins obtained by subtracting the total protein fraction with the non-adsorbed protein fraction).[69,73] For each isotherm, a set of samples containing a constant concentration of NPs (1 g L^{-1}) and varying concentrations of proteins (ranging from 0.01 to 2 g L^{-1}) was prepared. The samples were gently mixed at room temperature for 3 h and then centrifuged (20,000 g, 10 min). Protein concentration in the supernatant was finally measured by spectrophotometry. The affinity constants were calculated by fitting the adsorption isotherms to the Langmuir model[97] according to **Equation (1)**:

$$m_{ads} = \frac{m_{\infty}.K_{ads}.C}{1+K_{ads}.C} \quad (1)$$

where m_{ads} (mg m^{-2}) is the mass of adsorbed protein per square meter of NPs and C (g L^{-1}) is the non-adsorbed protein concentration at equilibrium. The deduced constants are m_{∞} (mg m^{-2}), the maximum amount of adsorbed protein per square meter of NPs, and K_{ads} (L mol^{-1}), the adsorption constant (proportional to the affinity) given in moles of subunits to account for the large size differences of the proteins studied. m_{ads} was converted into N_{ads} (number of proteins per NP) for comparison purposes.

Isothermal Titration Calorimetry (ITC)

ITC of hemoproteins adsorbed on silica NPs was performed using a VP-ITC calorimeter (MicroCal). Before each measurement, every solution was degassed under vacuum. The reaction cell (1.8 mL) was loaded with a NP solution and the syringe (500 µL) was filled with a hemoprotein solution. NP and protein concentrations varied from 1 to 10 g L^{-1} and 0.01 to 0.3 mmol L^{-1}, respectively. The proteins and NPs were prepared in the same buffer (phosphate, 0.1 mol L^{-1}, pH 6 or 7) to prevent any pH effect. The experiments were done in triplicate at 20 °C by adding 10 µL of the protein solution to the NP solution with an equilibration interval of 350 s. The control experiments were performed either without protein or without NPs. The measured heat exchange was subtracted from the titration data prior to curve-fitting. The enthalpy (ΔH), the stoichiometry of the reaction (N_I), and the association constant (K_{ads}) were obtained by nonlinear least-squares fitting of the experimental data using the single set of independent binding sites (SSIS) model[98] of the Origin software provided with the instrument.

UV Circular Dichroism (CD)

The CD study was done using a Chirascan spectrometer (Applied Photophysics). Because the CD signal is proportional to the amount of protein secondary structures, subunit concentration was kept constant for every hemoprotein, at 3 µmol L^{-1}. NP concentrations were calculated from the

adsorption isotherm data in order to obtain a large excess of adsorbed protein in solution (80% for Mb, 90% for Hb, and 70% for HbC1 and HbAm). The final NP concentration ranged from 1 to 20 g L^{-1}. Samples were placed in phosphate buffer (0.1 mol L^{-1}, pH 7) and gently mixed for 3 h before measurements. We used 1 mm Quartz cells (Hellma), requiring a volume of 400 µL. Spectra were measured from 190 to 250 nm with 0.5 nm steps and 0.5 s of acquisition time per point. Dichroic signals were corrected by the NP-buffered solution spectrum, which showed no significant signal in the range of wavelengths studied (**Figure S7**). Measured ellipticity was converted into delta epsilon ($\Delta\varepsilon$) by normalizing with the subunit molar concentration (3 µmol L^{-1}), the number of residues per subunit (153, 144, 146, and 176 residues, respectively), and the pathlength (0.1 cm). Normalization was done using the BeStSel web server.[99]

Cryogenic Transmission Electron Microscopy (cryo-TEM)

Solutions containing HbAm proteins and silica NPs in phosphate buffer (0.1 mol L^{-1}, pH 6 or 7) were prepared as follows: concentrations were chosen so as to obtain more than 80% of adsorbed proteins (excess of NPs); C_{HbAm} = 0.4 g L^{-1}; C_{NP} = 3 or 6 g L^{-1} (pH 6 and 7, respectively). Then, 4 µL of sample solution was deposited onto a glow-discharged holey carbon grid (Quantifoil R2/2). The grid was blotted with filter paper for 2 s and directly plunged into liquid ethane cooled by liquid nitrogen using a Vitrobot Mark IV (Thermo Fisher Scientific) operated at 22 °C and 100% relative humidity. The grids were stored in liquid nitrogen until use. Frozen samples were transferred to a Gatan 626 cryo-holder and observed in a JEOL 2010F cryo transmission electron microscope operating at 200 kV. The samples were imaged with a magnification of ×50,000 using a minimal dose system and the images were collected with a Gatan Ultrascan 4K CCD camera at a 2.7 µm of nominal defocus.

ASSOCIATED CONTENT

The following sections are available free of charge in the **Supporting Information** file at https://pubs.acs.org/:

Figure S1: Scale representation of the structures of hemoproteins

Figure S2: Absorption spectra of hemoproteins

Figure S3: Size-exclusion chromatography of annelid coelom and blood

Figure S4: Small-angle neutron scattering curves of hemoprotein solutions

Figure S5: Structural characterization of LUDOX TM-50 silica nanoparticles.

Figure S6: Isothermal titration calorimetry experiments of hemoproteins adsorbed on silica NPs (pH 6)

Figure S7: Circular dichroism spectra of free hemoproteins and silica nanoparticles

Figure S8: Distribution of the orientations of HbAm interacting with nanoparticles

Table S1: Adsorption and thermodynamic constants of hemoproteins adsorbed on silica nanoparticles

AUTHOR INFORMATION

Corresponding Authors

Laurent Marichal*: marichal.laurent@hotmail.com

Serge Pin*: serge.pin@cea.fr

Author Contributions

The manuscript was written with contributions from all authors. All authors approved the final version of the manuscript.

Conflict of Interest: The authors declare no competing financial interest.

ACKNOWLEDGMENTS

The authors are grateful to Jean Labarre (CEA) for his scientific contribution and his supervision of L. Marichal during his PhD thesis.

Funding Sources

This research was supported by a grant from the CEA "*Programme de Toxicologie"* (NaToM grant).

L. Marichal was supported by a CFR grant from the CEA.

The MESCAL cruise during which *Riftia pachyptila* specimens were collected was supported by the Flotte Océanographique Française.

This work was supported by the French Infrastructure for Integrated Structural Biology (FRISBI) ANR-10-INBS-05.

The electron microscopy imaging was supported by "*Investissements d'Avenir*" LabEx PALM (ANR-10LABX-0039-PALM).

The authors are grateful to the French METSA network (FR3507) for their financial support for the cryo-TEM experiments.

REFERENCES

(1) Freundlich, H. Über Die Adsorption in Lösungen. *Zeitschrift für Phys. Chemie* **1907**, *57U* (1). https://doi.org/10.1515/zpch-1907-5723.

(2) Abramson, H. A. ELECTROKINETIC PHENOMENA: VI. RELATIONSHIP BETWEEN ELECTRIC MOBILITY, CHARGE, AND TITRATION OF PROTEINS. *J. Gen. Physiol.* **1932**, *15* (5), 575–603. https://doi.org/10.1085/jgp.15.5.575.

(3) Parak, W. J.; Nel, A. E.; Weiss, P. S. Grand Challenges for Nanoscience and

Nanotechnology. *ACS Nano* **2015**, *9* (7), 6637–6640. https://doi.org/10.1021/acsnano.5b04386.

(4) Vance, M. E.; Kuiken, T.; Vejerano, E. P.; McGinnis, S. P.; Hochella, M. F.; Rejeski, D.; Hull, M. S. Nanotechnology in the Real World: Redeveloping the Nanomaterial Consumer Products Inventory. *Beilstein J. Nanotechnol.* **2015**, *6* (1), 1769–1780. https://doi.org/10.3762/bjnano.6.181.

(5) Kagan, C. R.; Fernandez, L. E.; Gogotsi, Y.; Hammond, P. T.; Hersam, M. C.; Nel, A. E.; Penner, R. M.; Willson, C. G.; Weiss, P. S. Nano Day: Celebrating the Next Decade of Nanoscience and Nanotechnology. *ACS Nano* **2016**, *10* (10), 9093–9103. https://doi.org/10.1021/acsnano.6b06655.

(6) Anselmo, A. C.; Mitragotri, S. Nanoparticles in the Clinic. *Bioeng. Transl. Med.* **2016**, *1* (1), 10–29. https://doi.org/10.1002/btm2.10003.

(7) Pelaz, B.; Alexiou, C.; Alvarez-Puebla, R. A.; Alves, F.; Andrews, A. M.; Ashraf, S.; Balogh, L. P.; Ballerini, L.; Bestetti, A.; Brendel, C.; Bosi, S.; Carril, M.; Chan, W. C. W.; Chen, C.; Chen, X.; Chen, X.; Cheng, Z.; Cui, D.; Du, J.; Dullin, C.; Escudero, A.; Feliu, N.; Gao, M.; George, M.; Gogotsi, Y.; Grünweller, A.; Gu, Z.; Halas, N. J.; Hampp, N.; Hartmann, R. K.; Hersam, M. C.; Hunziker, P.; Jian, J.; Jiang, X.; Jungebluth, P.; Kadhiresan, P.; Kataoka, K.; Khademhosseini, A.; Kopeček, J.; Kotov, N. A.; Krug, H. F.; Lee, D. S.; Lehr, C.-M.; Leong, K. W.; Liang, X.-J.; Ling Lim, M.; Liz-Marzán, L. M.; Ma, X.; Macchiarini, P.; Meng, H.; Möhwald, H.; Mulvaney, P.; Nel, A. E.; Nie, S.; Nordlander, P.; Okano, T.; Oliveira, J.; Park, T. H.; Penner, R. M.; Prato, M.; Puntes, V.; Rotello, V. M.; Samarakoon, A.; Schaak, R. E.; Shen, Y.; Sjöqvist, S.; Skirtach, A. G.; Soliman, M. G.; Stevens, M. M.; Sung, H.-W.; Tang, B. Z.; Tietze, R.; Udugama, B. N.; VanEpps, J. S.; Weil, T.; Weiss, P. S.; Willner, I.; Wu, Y.; Yang, L.; Yue, Z.; Zhang, Q.; Zhang, Q.; Zhang, X.-E.; Zhao, Y.; Zhou, X.; Parak, W. J. Diverse Applications of Nanomedicine. *ACS Nano* **2017**, *11* (3), 2313–2381. https://doi.org/10.1021/acsnano.6b06040.

(8) Hua, S.; de Matos, M. B. C.; Metselaar, J. M.; Storm, G. Current Trends and Challenges in the Clinical Translation of Nanoparticulate Nanomedicines: Pathways for Translational Development and Commercialization. *Front. Pharmacol.* **2018**, *9* (JUL), 1–14. https://doi.org/10.3389/fphar.2018.00790.

(9) Soares, S.; Sousa, J.; Pais, A.; Vitorino, C. Nanomedicine: Principles, Properties, and Regulatory Issues. *Front. Chem.* **2018**, *6* (AUG), 1–15. https://doi.org/10.3389/fchem.2018.00360.

(10) Rivera Gil, P.; Oberdörster, G.; Elder, A.; Puntes, V.; Parak, W. J. Correlating Physico-Chemical with Toxicological Properties of Nanoparticles: The Present and the Future. *ACS Nano* **2010**, *4* (10), 5527–5531. https://doi.org/10.1021/nn1025687.

(11) Sharifi, S.; Behzadi, S.; Laurent, S.; Laird Forrest, M.; Stroeve, P.; Mahmoudi, M. Toxicity of Nanomaterials. *Chem. Soc. Rev.* **2012**, *41* (6), 2323–2343. https://doi.org/10.1039/C1CS15188F.

(12) Shin, S.; Song, I.; Um, S. Role of Physicochemical Properties in Nanoparticle Toxicity.

Nanomaterials **2015**, *5* (3), 1351–1365. https://doi.org/10.3390/nano5031351.

(13) Su, H.; Wang, Y.; Gu, Y.; Bowman, L.; Zhao, J.; Ding, M. Potential Applications and Human Biosafety of Nanomaterials Used in Nanomedicine. *J. Appl. Toxicol.* **2018**, *38* (1), 3–24. https://doi.org/10.1002/jat.3476.

(14) Monopoli, M. P.; Åberg, C.; Salvati, A.; Dawson, K. A. Biomolecular Coronas Provide the Biological Identity of Nanosized Materials. *Nat. Nanotechnol.* **2012**, *7* (12), 779–786. https://doi.org/10.1038/nnano.2012.207.

(15) Kelly, P. M.; Åberg, C.; Polo, E.; O'Connell, A.; Cookman, J.; Fallon, J.; Krpetić, Ž.; Dawson, K. a. Mapping Protein Binding Sites on the Biomolecular Corona of Nanoparticles. *Nat. Nanotechnol.* **2015**, *10* (5), 472–479. https://doi.org/10.1038/nnano.2015.47.

(16) Docter, D.; Westmeier, D.; Markiewicz, M.; Stolte, S.; Knauer, S. K.; Stauber, R. H. The Nanoparticle Biomolecule Corona: Lessons Learned – Challenge Accepted? *Chem. Soc. Rev.* **2015**, *44* (17), 6094–6121. https://doi.org/10.1039/C5CS00217F.

(17) Baimanov, D.; Cai, R.; Chen, C. Understanding the Chemical Nature of Nanoparticle–Protein Interactions. *Bioconjug. Chem.* **2019**, *30* (7), 1923–1937. https://doi.org/10.1021/acs.bioconjchem.9b00348.

(18) Peng, Q.; Liu, J.; Zhang, T.; Zhang, T.-X.; Zhang, C.-L.; Mu, H. Digestive Enzyme Corona Formed in the Gastrointestinal Tract and Its Impact on Epithelial Cell Uptake of Nanoparticles. *Biomacromolecules* **2019**, *20* (4), 1789–1797. https://doi.org/10.1021/acs.biomac.9b00175.

(19) Cai, R.; Chen, C. The Crown and the Scepter: Roles of the Protein Corona in Nanomedicine. *Adv. Mater.* **2019**, *31* (45), 1805740. https://doi.org/10.1002/adma.201805740.

(20) Francia, V.; Yang, K.; Deville, S.; Reker-Smit, C.; Nelissen, I.; Salvati, A. Corona Composition Can Affect the Mechanisms Cells Use to Internalize Nanoparticles. *ACS Nano* **2019**, *13* (10), 11107–11121. https://doi.org/10.1021/acsnano.9b03824.

(21) Zoungrana, T.; Findenegg, G. H.; Norde, W. Structure, Stability, and Activity of Adsorbed Enzymes. *J. Colloid Interface Sci.* **1997**, *190* (2), 437–448. https://doi.org/10.1006/jcis.1997.4895.

(22) Cukalevski, R.; Lundqvist, M.; Oslakovic, C.; Dahlbäck, B.; Linse, S.; Cedervall, T. Structural Changes in Apolipoproteins Bound to Nanoparticles. *Langmuir* **2011**, *27* (23), 14360–14369. https://doi.org/10.1021/la203290a.

(23) Klein, G.; Devineau, S.; Aude, J. C.; Boulard, Y.; Pasquier, H.; Labarre, J.; Pin, S.; Renault, J. P. Interferences of Silica Nanoparticles in Green Fluorescent Protein Folding Processes. *Langmuir* **2016**, *32* (1), 195–202. https://doi.org/10.1021/acs.langmuir.5b03890.

(24) Johnson, B. J.; Russ Algar, W.; Malanoski, A. P.; Ancona, M. G.; Medintz, I. L. Understanding Enzymatic Acceleration at Nanoparticle Interfaces: Approaches and Challenges. *Nano Today* **2014**, *9* (1), 102–131.

https://doi.org/10.1016/j.nantod.2014.02.005.

(25) Wei, Y.; Thyparambil, A. A.; Wu, Y.; Latour, R. A. Adsorption-Induced Changes in Ribonuclease A Structure and Enzymatic Activity on Solid Surfaces. *Langmuir* **2014**, *30* (49), 14849–14858. https://doi.org/10.1021/la503854a.

(26) Devineau, S.; Kiger, L.; Galacteros, F.; Baudin-Creuza, V.; Marden, M.; Renault, J. P.; Pin, S. Manipulating Hemoglobin Oxygenation Using Silica Nanoparticles: A Novel Prospect for Artificial Oxygen Carriers. *Blood Adv.* **2018**, *2* (2), 90–94. https://doi.org/10.1182/bloodadvances.2017012153.

(27) Patel, P.; Kumar, A. CHAPTER 3. Factors Affecting a Nanoparticle's Protein Corona Formation; Kumar, A., Dhawan, A., Eds.; Issues in Toxicology; Royal Society of Chemistry: Cambridge, 2019; pp 61–79. https://doi.org/10.1039/9781788016308-00061.

(28) Mu, Q.; Jiang, G.; Chen, L.; Zhou, H.; Fourches, D.; Tropsha, A.; Yan, B. Chemical Basis of Interactions Between Engineered Nanoparticles and Biological Systems. *Chem. Rev.* **2014**, *114* (15), 7740–7781. https://doi.org/10.1021/cr400295a.

(29) Pulido-Reyes, G.; Leganes, F.; Fernández-Piñas, F.; Rosal, R. Bio-Nano Interface and Environment: A Critical Review. *Environ. Toxicol. Chem.* **2017**, *36* (12), 3181–3193. https://doi.org/10.1002/etc.3924.

(30) Nguyen, V. H.; Lee, B.-J. Protein Corona: A New Approach for Nanomedicine Design. *Int. J. Nanomedicine* **2017**, *Volume 12*, 3137–3151. https://doi.org/10.2147/IJN.S129300.

(31) Vertegel, A. A.; Siegel, R. W.; Dordick, J. S. Silica Nanoparticle Size Influences the Structure and Enzymatic Activity of Adsorbed Lysozyme. *Langmuir* **2004**, *20* (16), 6800–6807. https://doi.org/10.1021/la0497200.

(32) Lundqvist, M.; Stigler, J.; Elia, G.; Lynch, I.; Cedervall, T.; Dawson, K. A. Nanoparticle Size and Surface Properties Determine the Protein Corona with Possible Implications for Biological Impacts. *Proc. Natl. Acad. Sci. U. S. A.* **2008**, *105* (38), 14265–14270. https://doi.org/10.1073/pnas.0805135105.

(33) Piella, J.; Bastús, N. G.; Puntes, V. Size-Dependent Protein–Nanoparticle Interactions in Citrate-Stabilized Gold Nanoparticles: The Emergence of the Protein Corona. *Bioconjug. Chem.* **2017**, *28* (1), 88–97. https://doi.org/10.1021/acs.bioconjchem.6b00575.

(34) Marichal; Klein; Armengaud; Boulard; Chédin; Labarre; Pin; Renault; Aude. Protein Corona Composition of Silica Nanoparticles in Complex Media: Nanoparticle Size Does Not Matter. *Nanomaterials* **2020**, *10* (2), 240. https://doi.org/10.3390/nano10020240.

(35) Mathé, C.; Devineau, S.; Aude, J.-C.; Lagniel, G.; Chédin, S.; Legros, V.; Mathon, M.-H.; Renault, J.-P.; Pin, S.; Boulard, Y.; Labarre, J. Structural Determinants for Protein Adsorption/Non-Adsorption to Silica Surface. *PLoS One* **2013**, *8* (11), e81346. https://doi.org/10.1371/journal.pone.0081346.

(36) Tenzer, S.; Docter, D.; Rosfa, S.; Wlodarski, A.; Kuharev, J.; Rekik, A.; Knauer, S. K.; Bantz, C.; Nawroth, T.; Bier, C.; Sirirattanapan, J.; Mann, W.; Treuel, L.; Zellner, R.;

Maskos, M.; Schild, H.; Stauber, R. H. Nanoparticle Size Is a Critical Physicochemical Determinant of the Human Blood Plasma Corona: A Comprehensive Quantitative Proteomic Analysis. *ACS Nano* **2011**, *5* (9), 7155–7167. https://doi.org/10.1021/nn201950e.

(37) Cai, X.; Ramalingam, R.; Wong, H. S.; Cheng, J.; Ajuh, P.; Cheng, S. H.; Lam, Y. W. Characterization of Carbon Nanotube Protein Corona by Using Quantitative Proteomics. *Nanomedicine Nanotechnology, Biol. Med.* **2013**, *9* (5), 583–593. https://doi.org/10.1016/j.nano.2012.09.004.

(38) Klein, G.; Mathé, C.; Biola-Clier, M.; Devineau, S.; Drouineau, E.; Hatem, E.; Marichal, L.; Alonso, B.; Gaillard, J.-C.; Lagniel, G.; Armengaud, J.; Carrière, M.; Chédin, S.; Boulard, Y.; Pin, S.; Renault, J.-P.; Aude, J.-C.; Labarre, J. RNA-Binding Proteins Are a Major Target of Silica Nanoparticles in Cell Extracts. *Nanotoxicology* **2016**, *10* (10), 1555–1564. https://doi.org/10.1080/17435390.2016.1244299.

(39) Bharti, B.; Meissner, J.; Klapp, S. H. L.; Findenegg, G. H. Bridging Interactions of Proteins with Silica Nanoparticles: The Influence of PH, Ionic Strength and Protein Concentration. *Soft Matter* **2014**, *10* (5), 718–728. https://doi.org/10.1039/C3SM52401A.

(40) Devineau, S.; Zargarian, L.; Renault, J. P.; Pin, S. Structure and Function of Adsorbed Hemoglobin on Silica Nanoparticles: Relationship between the Adsorption Process and the Oxygen Binding Properties. *Langmuir* **2017**, *33* (13), 3241–3252. https://doi.org/10.1021/acs.langmuir.6b04281.

(41) Meissner, J.; Wu, Y.; Jestin, J.; Shelton, W. A.; Findenegg, G. H.; Bharti, B. PH-Induced Reorientation of Cytochrome c on Silica Nanoparticles. *Soft Matter* **2019**, *15* (3), 350–354. https://doi.org/10.1039/C8SM01909F.

(42) Rechendorff, K.; Hovgaard, M. B.; Foss, M.; Zhdanov, V. P.; Besenbacher, F. Enhancement of Protein Adsorption Induced by Surface Roughness. *Langmuir* **2006**, *22* (26), 10885–10888. https://doi.org/10.1021/la0621923.

(43) Pozzi, D.; Caracciolo, G.; Digiacomo, L.; Colapicchioni, V.; Palchetti, S.; Capriotti, A. L.; Cavaliere, C.; Zenezini Chiozzi, R.; Puglisi, A.; Laganà, A. The Biomolecular Corona of Nanoparticles in Circulating Biological Media. *Nanoscale* **2015**, *7* (33), 13958–13966. https://doi.org/10.1039/C5NR03701H.

(44) Mahmoudi, M.; Abdelmonem, A. M.; Behzadi, S.; Clement, J. H.; Dutz, S.; Ejtehadi, M. R.; Hartmann, R.; Kantner, K.; Linne, U.; Maffre, P.; Metzler, S.; Moghadam, M. K.; Pfeiffer, C.; Rezaei, M.; Ruiz-Lozano, P.; Serpooshan, V.; Shokrgozar, M. a.; Nienhaus, G. U.; Parak, W. J. Temperature: The "Ignored" Factor at the NanoBio Interface. *ACS Nano* **2013**, *7* (8), 6555–6562. https://doi.org/10.1021/nn305337c.

(45) Nel, A. E.; Mädler, L.; Velegol, D.; Xia, T.; Hoek, E. M. V; Somasundaran, P.; Klaessig, F.; Castranova, V.; Thompson, M. Understanding Biophysicochemical Interactions at the Nano-Bio Interface. *Nat. Mater.* **2009**, *8* (7), 543–557. https://doi.org/10.1038/nmat2442.

(46) Norde, W. My Voyage of Discovery to Proteins in Flatland …and Beyond. *Colloids*

Surfaces B Biointerfaces **2008**, *61* (1), 1–9. https://doi.org/10.1016/j.colsurfb.2007.09.029.

(47) Vogler, E. A. Protein Adsorption in Three Dimensions. *Biomaterials* **2012**, *33* (5), 1201–1237. https://doi.org/10.1016/j.biomaterials.2011.10.059.

(48) Rabe, M.; Verdes, D.; Seeger, S. Understanding Protein Adsorption Phenomena at Solid Surfaces. *Adv. Colloid Interface Sci.* **2011**, *162* (1–2), 87–106. https://doi.org/10.1016/j.cis.2010.12.007.

(49) Vroman, L. When Blood Is Touched. *Materials (Basel).* **2009**, *2* (4), 1547–1557. https://doi.org/10.3390/ma2041547.

(50) Antonini, E.; Brunori, M. *Hemoglobin and Myoglobin in Their Interactions with Ligands*, Frontiers.; North-Holland Pub. Co.: Amsterdam, 1971.

(51) Zal, F.; Lallier, F. H.; Green, B. N.; Vinogradov, S. N.; Toulmond, A. The Multi-Hemoglobin System of the Hydrothermal Vent Tube Worm Riftia Pachyptila. *J. Biol. Chem.* **1996**, *271* (15), 8875–8881. https://doi.org/10.1074/jbc.271.15.8875.

(52) Zal, F.; Green, B. N.; Lallier, F. H.; Vinogradov, S. N.; Toulmond, A. Quaternary Structure of the Extracellular Haemoglobin of the Lugworm Arenicola Marina. A Multi-Angle-Laser-Light-Scattering and Electrospray-Ionisation-Mass-Spectrometry Analysis. *Eur. J. Biochem.* **1997**, *243* (1–2), 85–92. https://doi.org/10.1111/j.1432-1033.1997.85_1a.x.

(53) Jouan, L.; Taveau, J.-C.; Marco, S.; Lallier, F. H.; Lamy, J. N. Occurrence of Two Architectural Types of Hexagonal Bilayer Hemoglobin in Annelids: Comparison of 3D Reconstruction Volumes of Arenicola Marina and Lumbricus Terrestris Hemoglobins. *J. Mol. Biol.* **2001**, *305* (4), 757–771. https://doi.org/10.1006/jmbi.2000.4344.

(54) Flores, J. F.; Fisher, C. R.; Carney, S. L.; Green, B. N.; Freytag, J. K.; Schaeffer, S. W.; Royer, W. E. Sulfide Binding Is Mediated by Zinc Ions Discovered in the Crystal Structure of a Hydrothermal Vent Tubeworm Hemoglobin. *Proc. Natl. Acad. Sci.* **2005**, *102* (8), 2713–2718. https://doi.org/10.1073/pnas.0407455102.

(55) de Godoy, L. M. F.; Olsen, J. V.; Cox, J.; Nielsen, M. L.; Hubner, N. C.; Fröhlich, F.; Walther, T. C.; Mann, M. Comprehensive Mass-Spectrometry-Based Proteome Quantification of Haploid versus Diploid Yeast. *Nature* **2008**, *455* (7217), 1251–1254. https://doi.org/10.1038/nature07341.

(56) Biörck, G. CHAPTER IV: Notes on the Chemistry of Myoglobin. *Acta Med. Scand.* **2009**, *133* (S226), 33–38. https://doi.org/10.1111/j.0954-6820.1949.tb11318.x.

(57) The Svedberg. SEDIMENTATION CONSTANTS, MOLECULAR WEIGHTS, AND ISOELECTRIC POINTS OF THE RESPIRATORY PROTEINS. *J. Biol. Chem.* **1933**, *103* (4), 311–325.

(58) Lazaro, A.; Vilanova, N.; Barreto Torres, L. D.; Resoort, G.; Voets, I. K.; Brouwers, H. J. H. Synthesis, Polymerization, and Assembly of Nanosilica Particles below the Isoelectric Point. *Langmuir* **2017**, *33* (51), 14618–14626. https://doi.org/10.1021/acs.langmuir.7b01498.

(59) Skoglund, S.; Hedberg, J.; Yunda, E.; Godymchuk, A.; Blomberg, E.; Odnevall Wallinder, I. Difficulties and Flaws in Performing Accurate Determinations of Zeta Potentials of Metal Nanoparticles in Complex Solutions—Four Case Studies. *PLoS One* **2017**, *12* (7), e0181735. https://doi.org/10.1371/journal.pone.0181735.

(60) Royer, W. E.; Omartian, M. N.; Knapp, J. E. Low Resolution Crystal Structure of Arenicola Erythrocruorin: Influence of Coiled Coils on the Architecture of a Megadalton Respiratory Protein. *J. Mol. Biol.* **2007**, *365* (1), 226–236. https://doi.org/10.1016/j.jmb.2006.10.016.

(61) Weber, R. E.; Vinogradov, S. N. Nonvertebrate Hemoglobins: Functions and Molecular Adaptations. *Physiol. Rev.* **2001**, *81* (2), 569–628. https://doi.org/10.1152/physrev.2001.81.2.569.

(62) Belato, F. A.; Schrago, C. G.; Coates, C. J.; Halanych, K. M.; Costa-Paiva, E. M. Newly Discovered Occurrences and Gene Tree of the Extracellular Globins and Linker Chains from the Giant Hexagonal Bilayer Hemoglobin in Metazoans. *Genome Biol. Evol.* **2019**, *11* (3), 597–612. https://doi.org/10.1093/gbe/evz012.

(63) Lesk, A. M.; Chothia, C. How Different Amino Acid Sequences Determine Similar Protein Structures: The Structure and Evolutionary Dynamics of the Globins. *J. Mol. Biol.* **1980**, *136* (3), 225–270. https://doi.org/10.1016/0022-2836(80)90373-3.

(64) Marichal, L.; Giraudon--Colas, G.; Cousin, F.; Thill, A.; Labarre, J.; Boulard, Y.; Aude, J.-C.; Pin, S.; Renault, J. P. Protein–Nanoparticle Interactions: What Are the Protein–Corona Thickness and Organization? *Langmuir* **2019**, *35* (33), 10831–10837. https://doi.org/10.1021/acs.langmuir.9b01373.

(65) Rimola, A.; Costa, D.; Sodupe, M.; Lambert, J.-F.; Ugliengo, P. Silica Surface Features and Their Role in the Adsorption of Biomolecules: Computational Modeling and Experiments. *Chem. Rev.* **2013**, *113* (6), 4216–4313. https://doi.org/10.1021/cr3003054.

(66) Byron, O.; Vestergaard, B. Protein–Protein Interactions: A Supra-Structural Phenomenon Demanding Trans-Disciplinary Biophysical Approaches. *Curr. Opin. Struct. Biol.* **2015**, *35*, 76–86. https://doi.org/10.1016/j.sbi.2015.09.003.

(67) Bekdemir, A.; Stellacci, F. A Centrifugation-Based Physicochemical Characterization Method for the Interaction between Proteins and Nanoparticles. *Nat. Commun.* **2016**, *7*, 1–8. https://doi.org/10.1038/ncomms13121.

(68) Weber, C.; Morsbach, S.; Landfester, K. Possibilities and Limitations of Different Separation Techniques for the Analysis of the Protein Corona. *Angew. Chemie Int. Ed.* **2019**, *58* (37), 12787–12794. https://doi.org/10.1002/anie.201902323.

(69) Goobes, R.; Goobes, G.; Campbell, C. T.; Stayton, P. S. Thermodynamics of Statherin Adsorption onto Hydroxyapatite †. *Biochemistry* **2006**, *45* (17), 5576–5586. https://doi.org/10.1021/bi052321z.

(70) Sulpizi, M.; Gaigeot, M.-P.; Sprik, M. The Silica–Water Interface: How the Silanols Determine the Surface Acidity and Modulate the Water Properties. *J. Chem. Theory*

Comput. **2012**, *8* (3), 1037–1047. https://doi.org/10.1021/ct2007154.

(71) Ohe, M.; Kajita, A. Changes in PKa Values of Individual Histidine Residues of Human Hemoglobin upon Reaction with Carbon Monoxide. *Biochemistry* **1980**, *19* (19), 4443–4450. https://doi.org/10.1021/bi00560a010.

(72) Cocco, M. J.; Kao, Y. H.; Phillips, A. T.; Lecomte, J. T. J. Structural Comparison of Apomyoglobin and Metaquomyoglobin: PH Titration of Histidines by NMR Spectroscopy. *Biochemistry* **1992**, *31* (28), 6481–6491. https://doi.org/10.1021/bi00143a018.

(73) Devineau, S.; Zanotti, J.-M.; Loupiac, C.; Zargarian, L.; Neiers, F.; Pin, S.; Renault, J. P. Myoglobin on Silica: A Case Study of the Impact of Adsorption on Protein Structure and Dynamics. *Langmuir* **2013**, *29* (44), 13465–13472. https://doi.org/10.1021/la4035479.

(74) Wang, J.; Jensen, U. B.; Jensen, G. V.; Shipovskov, S.; Balakrishnan, V. S.; Otzen, D.; Pedersen, J. S.; Besenbacher, F.; Sutherland, D. S. Soft Interactions at Nanoparticles Alter Protein Function and Conformation in a Size Dependent Manner. *Nano Lett.* **2011**, *11* (11), 4985–4991. https://doi.org/10.1021/nl202940k.

(75) Swenson, H.; Stadie, N. P. Langmuir's Theory of Adsorption: A Centennial Review. *Langmuir* **2019**, *35* (16), 5409–5426. https://doi.org/10.1021/acs.langmuir.9b00154.

(76) Thill, A.; Désert, A.; Fouilloux, S.; Taveau, J.-C.; Lambert, O.; Lansalot, M.; Bourgeat-Lami, E.; Spalla, O.; Belloni, L.; Ravaine, S.; Duguet, E. Spheres Growing on a Sphere: A Model to Predict the Morphology Yields of Colloidal Molecules Obtained through a Heterogeneous Nucleation Route. *Langmuir* **2012**, *28* (31), 11575–11583. https://doi.org/10.1021/la301857h.

(77) Tang, Z.; Palafox-Hernandez, J. P.; Law, W.-C.; Hughes, Z. E.; Swihart, M. T.; Prasad, P. N.; Knecht, M. R.; Walsh, T. R. Biomolecular Recognition Principles for Bionanocombinatorics: An Integrated Approach To Elucidate Enthalpic and Entropic Factors. *ACS Nano* **2013**, *7* (11), 9632–9646. https://doi.org/10.1021/nn404427y.

(78) Manoharan, V. N. Colloidal Matter: Packing, Geometry, and Entropy. *Science (80-.).* **2015**, *349* (6251), 1253751–1253751. https://doi.org/10.1126/science.1253751.

(79) Sprenger, K. G.; Pfaendtner, J. Strong Electrostatic Interactions Lead to Entropically Favorable Binding of Peptides to Charged Surfaces. *Langmuir* **2016**, *32* (22), 5690–5701. https://doi.org/10.1021/acs.langmuir.6b01296.

(80) Lynch, I.; Dawson, K. A. Protein-Nanoparticle Interactions. *Nano Today* **2008**, *3* (1–2), 40–47. https://doi.org/10.1016/S1748-0132(08)70014-8.

(81) Hunter, C. A.; Tomas, S. Cooperativity, Partially Bound States, and Enthalpy-Entropy Compensation. *Chem. Biol.* **2003**, *10* (11), 1023–1032. https://doi.org/10.1016/j.chembiol.2003.10.009.

(82) Bishop, K. J. M.; Wilmer, C. E.; Soh, S.; Grzybowski, B. A. Nanoscale Forces and Their Uses in Self-Assembly. *Small* **2009**, *5* (14), 1600–1630. https://doi.org/10.1002/smll.200900358.

(83) Holzwarth, G.; Doty, P. The Ultraviolet Circular Dichroism of Polypeptides 1. *J. Am. Chem. Soc.* **1965**, *87* (2), 218–228. https://doi.org/10.1021/ja01080a015.

(84) Cooper, T. M.; Woody, R. W. The Effect of Conformation on the CD of Interacting Helices: A Theoretical Study of Tropomyosin. *Biopolymers* **1990**, *30* (7–8), 657–676. https://doi.org/10.1002/bip.360300703.

(85) Lau, S. Y.; Taneja, A. K.; Hodges, R. S. Synthesis of a Model Protein of Defined Secondary and Quaternary Structure. Effect of Chain Length on the Stabilization and Formation of Two-Stranded Alpha-Helical Coiled-Coils. *J. Biol. Chem.* **1984**, *259* (21), 13253–13261.

(86) Graddis, T. J.; Myszka, D. G.; Chaiken, I. M. Controlled Formation of Model Homo- and Heterodimer Coiled Coil Polypeptides. *Biochemistry* **1993**, *32* (47), 12664–12671. https://doi.org/10.1021/bi00210a015.

(87) Mehboob, S.; Luo, B.-H.; Patel, B. M.; Fung, L. W.-M. Aβ Spectrin Coiled Coil Association at the Tetramerization Site †. *Biochemistry* **2001**, *40* (41), 12457–12464. https://doi.org/10.1021/bi010984k.

(88) Zheng, T.; Boyle, A.; Robson Marsden, H.; Valdink, D.; Martelli, G.; Raap, J.; Kros, A. Probing Coiled-Coil Assembly by Paramagnetic NMR Spectroscopy. *Org. Biomol. Chem.* **2015**, *13* (4), 1159–1168. https://doi.org/10.1039/C4OB02125H.

(89) Paulucci, A. A.; Hicks, L.; Machado, A.; Miranda, M. T. M.; Kay, C. M.; Farah, C. S. Specific Sequences Determine the Stability and Cooperativity of Folding of the C-Terminal Half of Tropomyosin. *J. Biol. Chem.* **2002**, *277* (42), 39574–39584. https://doi.org/10.1074/jbc.M204749200.

(90) *Encyclopedia of Surface and Colloid Science, Third Edition*; Somasundaran, P., Ed.; CRC Press, 2015. https://doi.org/10.1081/E-ESCS3.

(91) Cates, M. E. Entropy Stabilizes Open Crystals. *Nat. Mater.* **2013**, *12* (3), 179–180. https://doi.org/10.1038/nmat3573.

(92) Kihara, S.; van der Heijden, N. J.; Seal, C. K.; Mata, J. P.; Whitten, A. E.; Köper, I.; McGillivray, D. J. Soft and Hard Interactions between Polystyrene Nanoplastics and Human Serum Albumin Protein Corona. *Bioconjug. Chem.* **2019**, *30* (4), 1067–1076. https://doi.org/10.1021/acs.bioconjchem.9b00015.

(93) Wang, H.; Ma, R.; Nienhaus, K.; Nienhaus, G. U. Formation of a Monolayer Protein Corona around Polystyrene Nanoparticles and Implications for Nanoparticle Agglomeration. *Small* **2019**, *15* (22), 1900974. https://doi.org/10.1002/smll.201900974.

(94) Dominguez-Medina, S.; Kisley, L.; Tauzin, L. J.; Hoggard, A.; Shuang, B.; D. S. Indrasekara, A. S.; Chen, S.; Wang, L.-Y.; Derry, P. J.; Liopo, A.; Zubarev, E. R.; Landes, C. F.; Link, S. Adsorption and Unfolding of a Single Protein Triggers Nanoparticle Aggregation. *ACS Nano* **2016**, *10* (2), 2103–2112. https://doi.org/10.1021/acsnano.5b06439.

(95) Perutz, M. F. Preparation of Haemoglobin Crystals. *J. Cryst. Growth* **1968**, *2* (1), 54–56.

https://doi.org/10.1016/0022-0248(68)90071-7.

(96) Jelkmann, W.; Bauer, C. What Is the Best Method to Remove 2,3-Diphosphoglycerate from Hemoglobin? *Anal. Biochem.* **1976**, *75* (2), 382–388. https://doi.org/10.1016/0003-2697(76)90092-0.

(97) Langmuir, I. THE ADSORPTION OF GASES ON PLANE SURFACES OF GLASS, MICA AND PLATINUM. *J. Am. Chem. Soc.* **1918**, *40* (9), 1361–1403. https://doi.org/10.1021/ja02242a004.

(98) Welsch, N.; Becker, A. L.; Dzubiella, J.; Ballauff, M. Core–Shell Microgels as "Smart" Carriers for Enzymes. *Soft Matter* **2012**, *8* (5), 1428–1436. https://doi.org/10.1039/C1SM06894F.

(99) Micsonai, A.; Wien, F.; Bulyáki, É.; Kun, J.; Moussong, É.; Lee, Y.-H.; Goto, Y.; Réfrégiers, M.; Kardos, J. BeStSel: A Web Server for Accurate Protein Secondary Structure Prediction and Fold Recognition from the Circular Dichroism Spectra. *Nucleic Acids Res.* **2018**, *46* (W1), W315–W322. https://doi.org/10.1093/nar/gky497.